25·29 August 2024
inter.noise
NANTES FRANCE

On improving sound source localization in the wind tunnel

Christof Puhle[1]
Society for the Advancement of Applied Computer Science, GFaI e.V.
Volmerstraße 3, 12489 Berlin, Germany

ABSTRACT

When traveling in an open-jet wind tunnel, the path of an acoustic wave is affected by the flow causing a shift of source positions in acoustical maps of phased arrays outside the flow. In this paper, we start by comparing several well-known approaches to correct travel times between microphones and assumed sources, used, for example, by beamforming algorithms in such an environment. The methods under consideration include the original 1D-Amiet/Bahr formulation, a standard 2.5D-planar approach that assumes the constancy of angular frequency and wave-number-vector components along a plane, and finally, a 3D-ray-tracing method. Common to the former two of these methods is the assumption that the boundary layer of the flow, the so-called shear layer, is infinitely thin and refracts the acoustical ray, whereas, in principle, the latter algorithm allows for an arbitrary (but sufficiently smooth) vector field modeling the flow. Going through these methods, we discuss travel-time results relative to each other and in terms of differences in source localization using beamforming maps. In particular, we model the flow of an existing wind tunnel and discuss results of real-world measurements comparing the 2.5D-planar approach with the 3D-ray-tracing method.

1. REVIEW OF METHODS

1.1. One-dimensional shear-layer correction of Amiet

At its core, the shear-layer correction of Amiet (see [1, 2]) is an 1-dimensional method whose geometric concept the authors of [3] depict as in Figure 1. Under the assumption that the shear layer between the flow of mach number M and the flow-free region is infinitely thin and refracts the acoustical ray, Amiet derives relations between the lengths and angles involved when describing the positions of sender S and observer O relative to the shear layer. He then solves the resulting non-linear equations numerically using a shooting method. Eventually, Schlinker and Amiet (see [3]) applied this 1-dimensional approach to sources in a cylindrical flow field in order to correct phases and magnitudes of a microphone measurement. Later, this concept was generalized (see for example Bahr et al. [4]) to flow fields of rectangular cross section, i.e. piece-wise planar shear layers.

1.2. Quasi-three-dimensional shear-layer correction of Delfs

In the case of planar shear layers, however, Delfs' ansatz (see [5]) allows for a quasi-three-dimensional correction of travel times between sources and microphones. The underlying geometric concept is presented in Figure 2.

[1]puhle@gfai.de

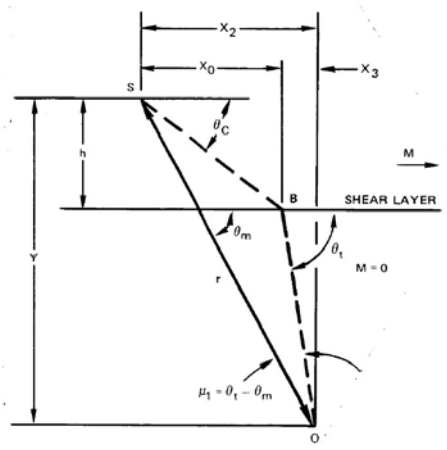

Figure 1: Geometric concept of 1-dimensional shear-layer correction of Amiet [3].

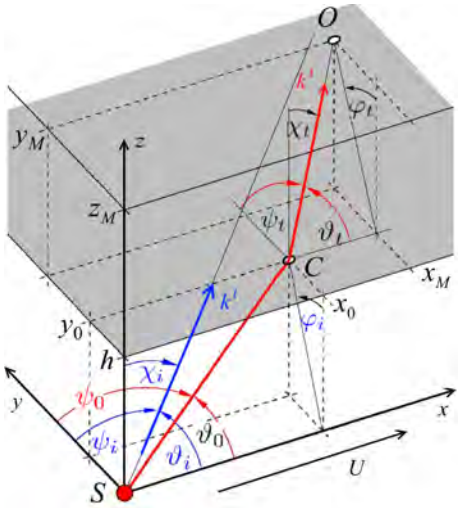

Figure 2: Geometric concept of quasi-three-dimensional shear-layer correction of Delfs [5].

As before, the shear layer is assumed to be infinitely thin and the wave front passing through it is approximated by a plane wave locally. In an analogy to optics, the main assumption of Delfs' model is the following: The x- and y-components of the wave vector k^i of the incoming plane wave remain constant when passing through the shear layer and the transmitted angular frequency ω^t takes up the spatial displacement of the Galilean transformation between stationary and moving coordinate systems, i.e.

$$\omega^i + U k_x^i = \omega^t, \tag{1}$$

$$k_x^i = k_x^t, \tag{2}$$

$$k_y^i = k_y^t. \tag{3}$$

A straightforward but lengthy computation (see [6] for a complete derivation) now yields a system of two non-linear equations for the angles ψ_t, ϑ_t (cf. Figure 2), which in turn uniquely determine the refraction point C for fixed positions of sender S and observer O.

1.3. Three-dimensional ray-tracing based methods

We now give a short introduction to a proper 3-dimensional method to determine/correct travel times in an open-jet wind tunnel - acoustical ray tracing. It utilizes the concept of a curved acoustic ray path moving along with a wave front as visualized in Figure 3 (see [7]).

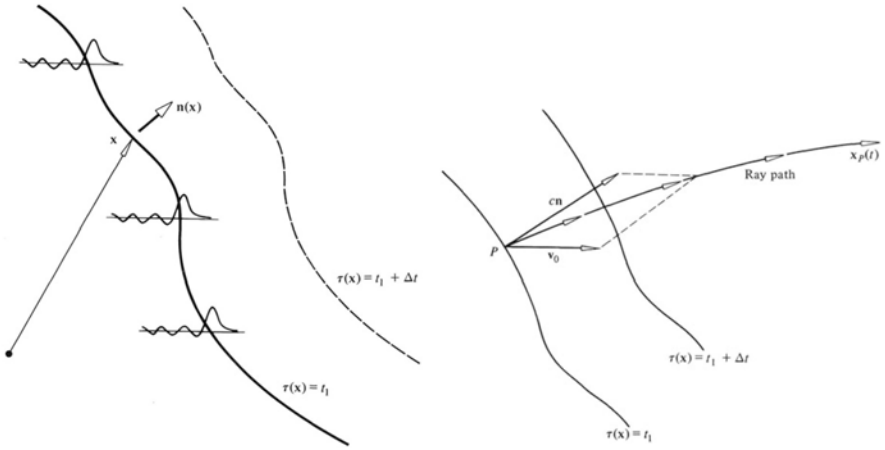

Figure 3: Concept of a curved acoustic ray path taken from Pierce [7].

We begin by defining the notion of wave front at the time t as the solution to the equation $t = \tau(x)$ for a given scalar field τ which encodes the propagation of the acoustical wave under consideration. Conversely, for any given point in space x, $\tau(x)$ is the instant of time at which the wave (packet) passes through x.

The gradient $s = \nabla\tau$ is called slowness vector field of τ, it is parallel to the normal n of the wave front (see Figure 3). However, when following an arbitrarily chosen point P on the wave front along its path $t \mapsto x_P(t)$ through a moving medium, neither s nor n are parallel to the velocity vector of x_P (cf. Figure 3). The components of x_P rather solve the following ordinary differential equations (see [7, 8]):

$$\frac{dx_i}{dt} = cn_i + v_i = \frac{c^2}{1 - \langle v, s\rangle} s_i + v_i, \quad i = 1,2,3. \tag{4}$$

Here, v denotes the velocity vector field of the moving medium, and c is the scalar field of propagation speed, both with respect to the coordinate system at rest and both not changing over time,

$$\frac{\partial c}{\partial t} = 0, \quad \frac{\partial v}{\partial t} = 0. \tag{5}$$

Moreover, all quantities on the right hand side of (4) are understood to be evaluated at $x(t)$ if they are a function of location.

Now, coming back to the problem discussed in this section, we are interested in solving system (4) starting from the location of source/sender, the latter processed in form of an initial condition for these ODEs. Although in principle there exists a unique solution for any sufficiently smooth fields v, s and c in this case, the slowness vector field s that contains the relevant information about τ seems to remain out of reach at this point of the consideration (if τ is not known beforehand). However, with the aid of the Eikonal equation, it is possible to derive first order ordinary differential equations – again along a path $t \mapsto x(t)$ – for the slowness vector field s as well (see [7, 8]):

$$\frac{ds_i}{dt} = \frac{\langle v, s\rangle - 1}{c} \frac{\partial c}{\partial x_i} - \sum_{j=1}^{3} s_j \frac{\partial v_j}{\partial x_i}, \quad i = 1,2,3. \tag{6}$$

Now, if provided with an initial value for both x and s there exists a unique solution to the ODE system (4), (6) for any fixed and sufficiently smooth fields v and c. In practice, it is only necessary to fix an initial direction for s, or equivalently, the wave front normal n, since the norm of s can be computed as

$$\|s\|_2 = |c + \langle v, n\rangle|^{-1}. \tag{7}$$

This approach allows for an iterative shooting method in order to connect sender S (or map point of a potential source in beamforming) and observer O (or microphone), and the resulting curved

acoustic ray provides all necessary information for phase and amplitude corrections. Alternatively, one could build up a grid of travel times and locations starting from S using this approach. In this case, phase and amplitude corrections for the microphone observer O are derived by computing a weighted average of the information available at the nearest grid points.

2. GENERALITY AND APPLICABILITY IN PRACTICE

Summarizing our considerations of the last section, it quickly becomes clear that the effort or complexity in order to generalize the one-dimensional approach of Amiet or the quasi-three-dimensional ansatz of Delfs to non-homogeneous flows of arbitrary shape is intractable. Although it seems imaginable – in certain situations – to linearize arbitrary flow shapes or to approximate the non-homogeneity of a flow by cascades of homogeneous flows, the numerical complexity of these kind of systems becomes higher or at least comparable to the introduced approach of acoustical ray tracing in the general case.

Initially, the ray-tracing approach seems hopeless to manage numerically as well, since in state of the art phased array systems 10^8 to 10^9 pairs of map and microphone locations have to be considered when computing a three-dimensional beamforming map of typical size. Sarradj took an important step towards the practicality of ray-tracing methods in this regard (see [9]). Instead of solving the initial value problem starting from every map point (of a high-resolution model), he reformulates the ODE system (4), (6) by performing a simple time reversal,

$$\bar{x}(t) = x(t_0 - t), \quad \bar{s}(t) = s(t_0 - t), \tag{8}$$

and solves the resulting system

$$\frac{d\bar{x}_i}{dt} = -\frac{c^2}{1 - \langle v, \bar{s}\rangle}\bar{s}_i - v_i, \quad \frac{d\bar{s}_i}{dt} = -\frac{\langle v, \bar{s}\rangle - 1}{c}\frac{\partial c}{\partial x_i} + \sum_{j=1}^{3} \bar{s}_j \frac{\partial v_j}{\partial x_i}, \quad i = 1,2,3, \tag{9}$$

starting from every microphone, a method we refer to as ray-back tracing here. Again, the right-hand side of (9) only depends on t by insertion of the time-reversed path $t \mapsto \bar{x}(t)$. By a variation of the initial values for $\bar{s}$, it is now possible to build up only one grid of travel times and locations of predetermined accuracy for every microphone that covers all map locations. A Delaunay triangulation together with barycentric coordinates of every cell then enables a quick interpolation of travel times for every map point inside the grid.

3. NUMERICAL COMPARISON OF TRAVEL TIMES

In this section, we compare numerical results of the ray-(back-)tracing method with those produced by the quasi-three-dimensional shear-layer correction of Delfs.

3.1. First numerical example

We begin to discuss a numerical example of a typical wind-tunnel setup. Let

$$v = U = (140,\ 0,\ 0)\ \text{km/h} \tag{10}$$

be the time-invariant, spatially homogeneous wind speed inside the flow,

$$c = 341.307\ \text{m/s} \tag{11}$$

is the everywhere constant speed of sound, the source/sender location is fixed at $S = (0,\ 0,\ 0)$ m, the observer/microphone location is

$$O = (-1.62949,\ 0.0740442,\ 4.17545)\ \text{m} \tag{12}$$

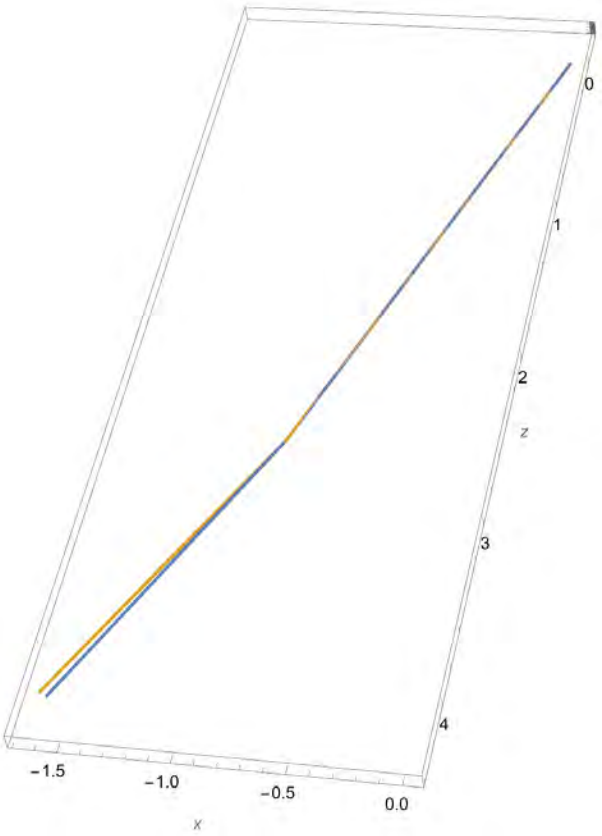

Figure 4: Comparison of the acoustic rays, quasi-three-dimensional shear-layer correction (yellow) and ray-tracing method (blue)

and the shear layer is determined by the equation $z = h = 2.63661$ m (cf. Figure 2). Then, the quasi-three-dimensional shear-layer correction determines the refraction point on the shear layer as

$$C = (-0.879717,\ 0.0457207,\ 2.63661)\ \text{m}. \tag{13}$$

Now, by solving the ray-tracing ODEs (4), (6) with the initial values

$$x(0) = S, \quad c\,n(0, x(0)) + v = \alpha(C - S), \quad \alpha > 0, \quad \|n(0, x(0))\| = 1, \tag{14}$$

we obtain the blue acoustic ray of Figure 4. Moreover, the acoustic ray of the quasi-three-dimensional shear-layer correction is visualized in yellow there. By definition, both acoustic rays coincide inside the flow and the yellow acoustic ray of the quasi-three-dimensional shear-layer correction ends at O in the flow-free region. However, at its nearest location O', the blue acoustic ray of the ray-tracing method misses O by 0.0394533 m. In particular, the corresponding difference $O - O'$ exhibits a non-trivial y-component. The resulting absolute value of the difference of the corresponding travel times Δt_{SO} and $\Delta t_{SO'}$ is

$$|\Delta t_{SO} - \Delta t_{SO'}| = 1.33087\ \mu\text{s}. \tag{15}$$

3.2. Ray-back tracing with Delaunay interpolation

We now apply the complete process of ray-back tracing together with a Delaunay interpolation as outlined in section 2 to an open-jet wind-tunnel setup which consists of $M = 192$ microphones arranged in a plane of dimension 3×5 m (see Figure 5). The corresponding shear-layer plane of the constant and homogeneous flow ($v = U = 140$ km/h) is perpendicular to the ground and rotated around the floor normal by 5° at a distance of 2 m to the center of the

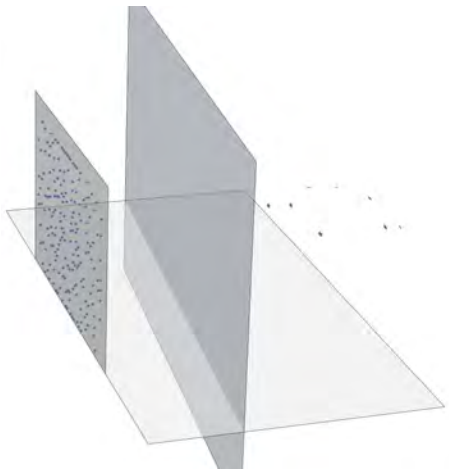

Figure 5: Wind-tunnel setup consisting of a 192-channel phased array, floor, shear-layer plane and a reduced 3D model (9 loudspeaker on a surface).

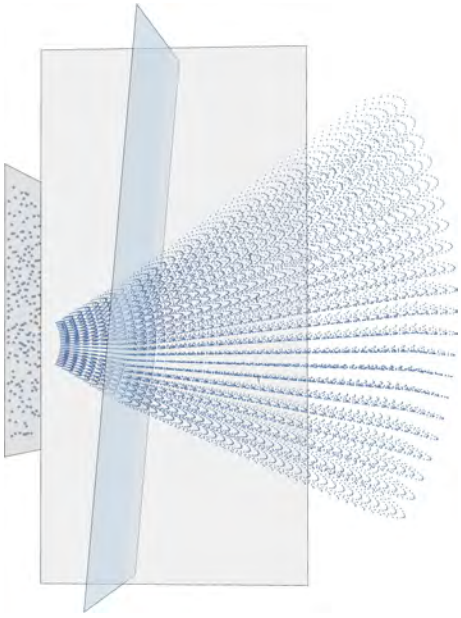

Figure 6: Sampling of acoustic ray paths obtained by ray-back tracing starting from an exemplary microphone

array. Moreover, all $N = 64239$ map points (9 loudspeaker on a surface) are located inside the flow (cf. Figure 5).

For every microphone, we then create a bundle of solutions to the ray-back-tracing ODEs (9) and discretize them such that every map point lies inside the corresponding three-dimensional Delaunay triangulation. An example bundle of sampled acoustic ray paths starting from one exemplary microphone can be found in Figure 6.

In the final step, for every map point in each of the M Delaunay triangulations, we determine its corresponding cell – a tetrahedron – and compute its (positive) barycentric coordinates with respect to the four vertices of the cell. These coordinates enable us to interpolate the travel time between the microphone and the map point by the four travel times of the vertices.

Let us denote by Δt_{ij}^R and Δt_{ij}^Q the travel times between the i-th microphone and the j-th map point computed using the above method of ray-back tracing with Delaunay interpolation and the quasi-three-dimensional shear-layer correction of Delfs, respectively. We then normalize

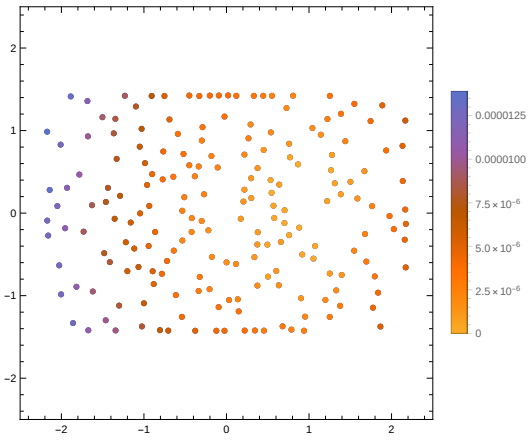

Figure 7: Average difference of travel times in s normalized with respect to a central reference microphone

these travel times with respect to a central reference microphone i_0,

$$d_{ij}^R = \Delta t_{ij}^R - \Delta t_{i_0 j}^R, \quad d_{ij}^Q = \Delta t_{ij}^Q - \Delta t_{i_0 j}^Q, \tag{16}$$

compute the average difference r_i between these normalized travel times,

$$r_i = \frac{1}{N} \sum_{j=1}^{N} \left| d_{ij}^R - d_{ij}^Q \right|, \quad i = 1, \ldots, M, \tag{17}$$

and visualize r_i at the corresponding microphone locations in Figure 7. As a consequence, the average difference r_i is well within the sampling duration in case of a 48 kHz-measurement.

4. REAL-WORLD MEASUREMENT AND AN INHOMOGENEOUS FLOW MODEL

In this section, we discuss the differences in source localization using beamforming maps when replacing the standard homogeneous flow model with a more realistic but inhomogeneous flow field.

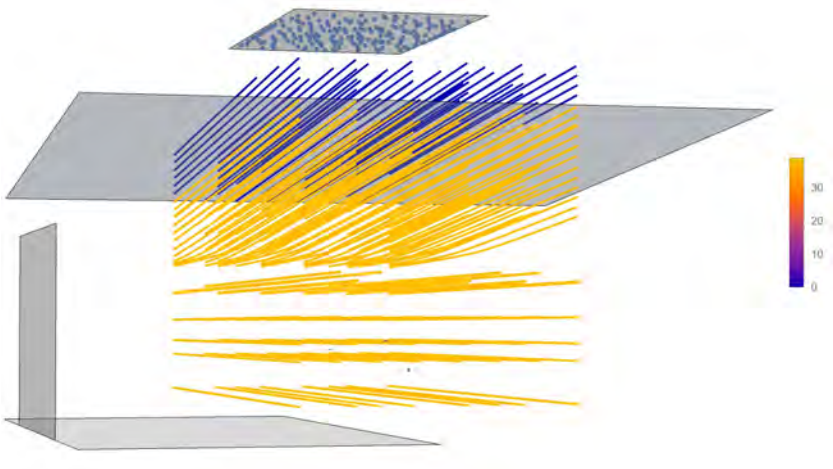

Figure 8: Inhomogeneous flow field in m/s, in a wind-tunnel setup consisting of an 192-channel phased top array, floor, shear-layer plane, side-array plane and a reduced 3D model (9 loudspeaker on a surface).

The homogeneous model used in this comparison is the quasi-three-dimensional shear-layer correction applied to a measurement of $M = 192$ microphones now placed on top of the

mapping region discussed before. Again, the shear-layer distance is 2 m and its widening angle is 5°. The competing inhomogeneous flow field is modeled to exhibit a central flow part parallel to the x-axis in the mapping region and to smoothly converge to the homogeneous flow field near the shear-layer (see Figure 8 for the complete setup). The described smooth transition was realized using the known switching function

$$\mathbb{R} \ni x \mapsto \frac{1}{\pi} \cdot \left(\arctan\left(-\frac{x}{\alpha} \right) + \frac{\pi}{2} \right) \in [0,1] \tag{18}$$

with the parameter

$$\alpha = 0.05, \tag{19}$$

and the size of central region was chosen as 1.5 m to include all map points. As practiced in section 3, we then determine the travel times necessary to compute a beamforming map using the method of ray-back tracing together with a Delaunay interpolation in this case.

Two measurements were taken, one without any flow in order to establish a ground truth for source locations and one with a flow speed of $v = U = 140$ km/h. Each measurement took 10 s using a sampling rate of 48 kHz. A fast Fourier transform with prior von Hann weighting was applied to every microphone signal using 50 % overlapping blocks of 4096 samples.

In each of the three cases (zero flow and non-trivial flow evaluated with homogeneous and inhomogeneous flow model), we computed a map using Functional Beamforming ($\nu = 8$) and determined the local maxima of the loudspeakers facing towards the top array (number 4, 5, 6), all of which were playing white noise. The results can be found in Table 1.

In terms of precision the inhomogeneous model performed better by far, and its accuracy is well within expected limits. However, the bias of the results suggest that accuracy could be improved even further by a calibration of the wind tunnel parameters, e.g. the shear-layer distance. Whether this is pure coincidence or a result of the more realistic flow model has to be cleared up in a follow-up investigation.

Table 1: Source locations determined using Functional Beamforming ($\nu = 8$).

Flow	**Model**	**Speaker**	**x in m**	**y in m**	**z in m**
0 km/h	–	4	-1.3276	-0.0581	0.0405
140 km/h	homog.	4	-1.3276 (±0.0000)	-0.0579 (+0.0002)	0.0325 (−0.0080)
140 km/h	inhomog.	4	-1.3301 (−0.0025)	-0.0583 (−0.0002)	0.0335 (−0.0070)
0 km/h	–	5	-0.0126	0.4280	0.0359
140 km/h	homog.	5	-0.0091 (+0.0035)	0.4283 (+0.0003)	0.0309 (−0.0050)
140 km/h	inhomog.	5	-0.0146 (−0.0020)	0.4279 (−0.0001)	0.0319 (−0.0040)
0 km/h	–	6	2.2303	0.0911	0.0577
140 km/h	homog.	6	2.2463 (+0.0160)	0.0970 (+0.0059)	0.0558 (−0.0019)
140 km/h	inhomog.	6	2.2283 (−0.0020)	0.0903 (−0.0008)	0.0577 (±0.0000)

ACKNOWLEDGMENTS

This research work has been funded by German Federal Ministry for Economic Affairs and Climate Action (Bundesministerium für Wirtschaft und Klimaschutz BMWK) under project *VeSuW* registration number 49VF210012.

REFERENCES

1. R.K. Amiet. Correction of open jet wind tunnel measurements for shear layer refraction. *American Institute of Aeronautics and Astronautics Paper No. 75-532*, 1975.
2. R.K. Amiet. Refraction of sound by a shear layer. *Journal of Sound and Vibration*, 58:467–482, 1978.
3. R. H. Schlinker and R. K. Amiet. Refraction and scattering of sound by a shear layer. In *Proceedings of the 6th aeroacoustics conference*. AIAA Paper 1980-973, 1980.
4. C. J. Bahr, T. F. Brooks, W. M. Humphreys, T. B. Spalt, and D. J. Stead. Acoustic data processing and transient signal analysis for the hybrid wing body 14-by 22-foot subsonic wind tunnel test. In *Proceedings of the 20th AIAA/CEAS aeroacoustics conference*. AIAA Paper 2014-2345, 2014.
5. J. Delfs. *Methoden der Aeroakustik*. lecture notes, spring semester, 2013.
6. C. Puhle. Über die Scherschichtkorrektur nach Amiet. technical report, Gesellschaft zur Förderung angewandter Informatik e.V., Berlin, Germany, 2015.
7. A.D. Pierce. *Acoustics*. Springer Cham, 2019.
8. R. Engelke. Ray trace acoustics in unsteady inhomogeneous flow. *J. Acoust. Soc. Am.*, 56:1291–1292, 1974.
9. E. Sarradj. A fast ray casting method for sound refraction at shear layers. In *Proceedings of the 22nd AIAA/CEAS aeroacoustics conference*. AIAA Paper 2016-2762, 2016.